



**HAL**  
open science

## Investigation of the Na<sub>2</sub>O/Ag<sub>2</sub>O ratio on the synthesis conditions and properties of the 80TeO<sub>2</sub>–10ZnO–[(10–x)Na<sub>2</sub>O–xAg<sub>2</sub>O] glasses

David Boiruchon, Frédéric Désévéday, Sébastien Chenu, Clément Strutynski, Frédéric Smektala, Grégory Gadret, Marc Dussauze, Veronique Jubera, Younès Messaddeq, Thierry Cardinal, et al.

### ► To cite this version:

David Boiruchon, Frédéric Désévéday, Sébastien Chenu, Clément Strutynski, Frédéric Smektala, et al.. Investigation of the Na<sub>2</sub>O/Ag<sub>2</sub>O ratio on the synthesis conditions and properties of the 80TeO<sub>2</sub>–10ZnO–[(10–x)Na<sub>2</sub>O–xAg<sub>2</sub>O] glasses. *Journal of Non-Crystalline Solids*, 2019, 525, 119691 (8 p.). 10.1016/j.jnoncrysol.2019.119691 . hal-02325521

**HAL Id: hal-02325521**

**<https://hal.science/hal-02325521v1>**

Submitted on 31 Oct 2019

**HAL** is a multi-disciplinary open access archive for the deposit and dissemination of scientific research documents, whether they are published or not. The documents may come from teaching and research institutions in France or abroad, or from public or private research centers.

L'archive ouverte pluridisciplinaire **HAL**, est destinée au dépôt et à la diffusion de documents scientifiques de niveau recherche, publiés ou non, émanant des établissements d'enseignement et de recherche français ou étrangers, des laboratoires publics ou privés.

# Investigation of the Na<sub>2</sub>O/Ag<sub>2</sub>O ratio on the synthesis conditions and properties of the 80TeO<sub>2</sub>-10ZnO-[(10-x)Na<sub>2</sub>O-xAg<sub>2</sub>O] glasses

Boiruchon D.<sup>1,5</sup>, Desevedavy F.<sup>2</sup>, Chenu S.<sup>3</sup>, Strutynski C.<sup>1</sup>, Smektala F.<sup>2</sup>, Gadret G.<sup>2</sup>, Dussauze M.<sup>4</sup>, Jubera V.<sup>1</sup>, Messaddeq Y.<sup>5</sup>, Cardinal Th.<sup>1</sup>, Danto S.<sup>1</sup>

<sup>1</sup>CNRS, Univ. Bordeaux, ICMCB, UMR 5026, F-33600 Pessac, France

<sup>2</sup>Laboratoire Interdisciplinaire Carnot de Bourgogne (ICB), UMR 6303 CNRS-Université de Bourgogne Franche-Comté, 9 Avenue Alain Savary, 21078 Dijon, France

<sup>3</sup>Institute of Research for Ceramics (IRCER), UMR 7315 CNRS-University of Limoges, 12 rue Atlantis, 87000 Limoges, France

<sup>4</sup>Institute of Molecular Science (ISM), UMR 5255 CNRS-University of Bordeaux, 33405 Talence, France

<sup>5</sup>Centre d'Optique, Photonique et Laser (COPL), Université Laval, Québec, QC, Canada

## ABSTRACT

Properties of the tellurite glasses 80TeO<sub>2</sub>-10ZnO-[(10-x)Na<sub>2</sub>O-xAg<sub>2</sub>O] are investigated as a function of the substitution ratio  $x$  between Na<sub>2</sub>O and Ag<sub>2</sub>O. One observe that the variation of glass transition temperature decreases monotonously with  $x$  and that surface crystallization mechanism is favored. The assignment of the Raman bands and their relation with the underlying glass structure is discussed. While both Na<sub>2</sub>O and Ag<sub>2</sub>O oxides act as glass network modifiers, their progressive equimolar substitution does not lead to a meaningful evolution in the structure of the TZ[Na<sub>10-x</sub>Ag<sub>x</sub>] glass. The refractive index and the cut-off wavelength are found to increase with  $x$ . The compositional and wavelength dependence of refractive indices, cut-off wavelength and optical band gap energy is discussed in terms of changes brought about by Na<sub>2</sub>O/Ag<sub>2</sub>O substitution in the glass network. Finally, it is shown that interaction between the platinum crucible and the glass melt increases with the silver content in the glass.

## 1. Introduction

Tellurium oxide based glasses own a wide optical transparency, ranging from the visible (~350 nm) up to 6  $\mu\text{m}$ , a good resistance to chemical attacks and crystallization, low phonon energy, a high rare earth ion solubility and a large third-order nonlinear susceptibility [1], [2], [3]. Owing to their properties, they are considered as attractive candidate to fill the strong demand for new integrated optical devices and laser amplifiers working in the mid-infrared regime, in planar or fiber optic forms [4], [5], [6], [7], [8], [9]. In the meantime, silver doping of glasses has appeared as an efficient route toward their functionalization with distinctive properties. As an example, Ag-doped chalcogenide glasses found applications as solid electrochemical sensors, waveguides, diffraction elements, optical memories and so on [[10]]. In phosphate glasses Ag insertion was considered for the direct Laser-inscription of optical elements in bulk and fiber forms [[11]], perennial recording [[12]] and for dosimetry [[13]]. In tellurite glasses, silver was considered mainly as a luminescence sensitizer of rare earth ions [14], [15]. It was investigated how silver nanoparticles can enhance the emission properties of rare earth doped tellurite glasses through an efficient surface plasmon resonance coupling [16]. Incorporation of silver nanoparticles in tellurite glasses was investigated as well for the improvement of their non-linear optical properties [[17]], leading to a substantial increase of optically stimulated second harmonic generation into ZnO-TeO<sub>2</sub> glass systems [[18],[19]]. The insertion of silver as nucleating agent was investigated to control the crystallization kinetics of tellurite glasses with homogeneously-dispersed sub-micron crystals to obtain transparent glass ceramics [[20]]. Finally Stepanov et al. [[21]] investigated the insertion of silver in tellurite for producing planar waveguides through Na<sup>+</sup>/Ag<sup>+</sup> ion exchange.

Here, one present a systematic investigation of the effect of the Na<sub>2</sub>O/Ag<sub>2</sub>O substitution on the properties of the host glass matrix 80TeO<sub>2</sub>-10ZnO-[(10-x)Na<sub>2</sub>O-xAg<sub>2</sub>O] (mol%) in the extensively studied ternary system TeO<sub>2</sub>-ZnO-Na<sub>2</sub>O [[5],[6],[8]]. One of the main issue in glass synthesis is the interaction of the melt with the crucible. The contamination of glass by platinum due to melting in crucibles has been extensively investigated, initially in phosphate glasses due to the need to procedure inclusion-free laser glasses with improved damage threshold [[22], [23], [24], [25]], but also in silica glasses [[26]] and tellurite glasses [[27], [28], [29]]. Although this effect is reported to affect optical properties of the glasses, the nature of the platinum species in the glass network remains to be elucidated. Here, by keeping the TeO<sub>2</sub> and ZnO molar concentrations fixed, one aim at discriminate the contribution of the two modifier oxides Na<sub>2</sub>O and Ag<sub>2</sub>O on important thermal, physical and optical properties of these glasses. Glass properties were investigated through differential scanning calorimetry (DSC), Raman spectroscopy and Fourier transform infrared (FTIR) spectroscopy. Material refractive index dispersion as a function of composition and wavelength were also measured. The observed evolution in cut-off wavelength ( $\lambda_c$ ) was correlated with the structural modification observed in the glass network with Na<sub>2</sub>O/Ag<sub>2</sub>O substitution. Inductively Coupled Plasma Emission Spectroscopy (ICP-OES) analysis were supported with luminescence measurements to quantify the chemical interactions occurring during the glass synthesis between the platinum crucible and the melt.

## 2. Experimental

The tellurium-zinc-sodium-silver glasses were synthesized using the standard melt-quench technique. Ten grams of high-purity precursors (TeO<sub>2</sub>: 5 N Strem, ZnO: 4 N Alfa Aesar, Na<sub>2</sub>CO<sub>3</sub>: 4 N Alfa Aesar, AgNO<sub>3</sub>: 5 N Alfa Aesar) were weighted in powder to get the required composition, grounded in a mortar and transferred in a platinum crucible. The mix was pre-heated at 150 °C for moisture removal, ramped up (10 °C.min<sup>-1</sup>) at 500 °C for 2 h, and then ramped up again at 750 °C for 15 min. Following the liquid was poured on a pre-heated brass plate to quench the melt. The melt was subjected twice to the same thermal cycle to ensure its complete homogeneity. Finally the bulk glass was annealed at ~T<sub>g</sub>-10 °C for 6 h before cooling to room temperature to release mechanical stress before sample grinding and polishing.

Thermal analysis was performed by TA Instruments AQ20 equipment. About 20 mg of glass in small pieces (~1-2 mm) was inserted into a Pt pan and placed in the chamber along with an empty reference pan. Characteristic temperatures were measured as the inflection point of the endotherm at a heating rate of 10 °C/min (precision  $\pm 3$  °C). The glass density ( $\rho$ ) was determined at room temperature by the Archimedes' method with an Alfa-Mirage MD-300S densimeter using diethyl phthalate as immersion liquid. The measurement precision was estimated to be  $\pm 0.02$  g/cm<sup>3</sup>.

Optical transmittance spectra in the UV-Vis wavelength range (200–3000 nm) were recorded on optically polished samples of about 2 mm thickness using a double-beam spectrophotometer (CARY 5000 Varian). Optical transmittance spectra in the near-IR wavelength range (1500–7500 nm) were recorded using a double-beam spectrophotometer (EQUINOX 55 Bruker). The linear refractive index measurements were carried out on polished glass slabs at three different wavelengths (633, 1064, and 1550 nm) by the means of a homemade prism ( $\text{TiO}_2$ ) coupler refractometer with an accuracy of  $\pm 0.005$ . Raman spectra were recorded with an Xplora Horiba micro-Raman spectrometer using a 785 nm excitation line with 10 mW of incident power. Raman spectra in the range of 200–1200  $\text{cm}^{-1}$  were recorded with a resolution of 2.5  $\text{cm}^{-1}$ .

Inductively conducted plasma-optical emission spectrometry (ICP/OES) was conducted with a Thermo Fisher Varian ICP/OES 720 ES apparatus. Luminescence spectroscopy has been investigated using an Edinburgh spectrometer equipped with double monochromators, Xenon lamp and cooled photomultiplier tube. Spectra were corrected to compensate the detector sensitivity and the flux of the lamp.

### 3. Results

The silver oxide fraction was increased from  $x = 0\%$  up to  $x = 10\%$  molar with the interval of 2% in the system  $80\text{TeO}_2\text{-}10\text{ZnO}\text{-}[(10-x)\text{Na}_2\text{O}\text{-}x\text{Ag}_2\text{O}]$  (series TZ[Na<sub>10-x</sub>Ag<sub>x</sub>]). The samples are classified accordingly to their level of Ag/Na substitution, from  $x = 0\%$  (TZ[Na<sub>10</sub>Ag<sub>0</sub>]) to  $x = 10\%$  (TZ[Na<sub>0</sub>Ag<sub>10</sub>]) respectively. Neither crystalline phase nor metallic silver nanoparticle formation could be evidenced under these experimental conditions.

Crystallization in tellurite glasses is a heterogeneous mechanism usually dominated by the surface. Only a few work report on the elaboration of transparent tellurite glass-ceramics containing a high crystalline volume fraction [[20]]. In order to investigate the potential role of silver as nucleating agent in TZN glasses DSC measurements were performed on bulk and powder samples. The DSC curves of the TZ[Na<sub>10-x</sub>Ag<sub>x</sub>] glasses are shown in Fig. 1a (bulk) and 1b (powder). Bulk measurements were made in small pieces of glass with  $\sim 1\text{-}2$  mm, while powder measurements were made using finely grinded samples.

The evolution of glass transition temperature  $T_g$  and of the onset crystallization temperature  $T_x$  for the glasses in bulk and powder forms along with their density  $\rho$  are reported on Table 1 and they are plotted in Fig. 2.

For both bulk and powder glass samples, only a slight and similar lowering of  $T_g$  with  $x$  is noticeable according to DSC measurements (Fig. 2a). Change however is clearly visible on crystallization peak positions. Considering bulk samples, the crystallization temperature  $T_{x1\text{-Bulk}}$  decreases monotonously with the increasing amount of  $\text{Ag}_2\text{O}$ . Similarly, the crystallization temperature  $T_{x1\text{-Powder}}$  decreases with  $x$ . However, in the case of the powder, the difference  $\Delta T = T_{x1} - T_g$  is reduced and one notice the appearance of a second crystallization peak ( $T_{x2\text{-Powder}}$ ), which might be due to the growth of a second crystalline phase. Finally, one observe that for  $x > 2$  the onset crystallization peak  $T_{x1\text{-Bulk}}$  and  $T_{x2\text{-Powder}}$  becomes very similar. One suggest that the first crystallization peak on powder is due to surface crystallization while the second one relates to bulk crystallization.

Density offers important insights on the structural modifications that occur in the samples with insertion of silver. The measured density  $\rho$  of the glasses TZ[Na<sub>10-x</sub>Ag<sub>x</sub>] are given in Table 1. The density is found to increase as a function of  $x$  (Fig. 2b), from  $\rho = 5.21 \text{ g.cm}^{-3}$  for  $x = 0\%$  (TZN) to  $\rho = 5.92 \text{ g.cm}^{-3}$  for  $x = 10\%$  (TZ[Na<sub>0</sub>Ag<sub>10</sub>]). Spontaneous Raman spectroscopy was carried out on the glasses TZ[Na<sub>10-x</sub>Ag<sub>x</sub>] in order to assess the structural deviation of the host glass matrix with silver content ( $\lambda_{\text{Excitation}} = 785 \text{ nm}$ ). The Raman signature of the glasses (normalized on the peak with the stronger intensity at 660  $\text{cm}^{-1}$ ) is depicted on Fig. 3.

The assignment of the Raman bands to structural elements for the glasses TZ[Na<sub>10-x</sub>Ag<sub>x</sub>] are dominated by five broad envelopes centered on 450  $\text{cm}^{-1}$ , 610  $\text{cm}^{-1}$ , 660  $\text{cm}^{-1}$ , 715  $\text{cm}^{-1}$  and 775  $\text{cm}^{-1}$  [[6]]. At lower wavenumber, the large envelopes peaking at 450  $\text{cm}^{-1}$  results from highly coupled symmetrical bending and stretching vibrational modes of the continuous [Te-O-Te] chains of corner sharing [TeO<sub>4</sub>], [TeO<sub>3</sub>] and [TeO<sub>3+1</sub>] polyhedra. The band located at 610  $\text{cm}^{-1}$  originates from anti-symmetric stretching of continuous networks composed of TeO<sub>4</sub> trigonal bipyramidal (tbp) sites. The high frequency modes at 660  $\text{cm}^{-1}$  are assigned to symmetric stretching of [TeO<sub>4</sub>] tbp units in the glass or to [Te-O-Te] linkage between two fourfold-coordinated Te atoms. The high energy bands at 715  $\text{cm}^{-1}$  and 775  $\text{cm}^{-1}$  are attributed to the stretching vibration modes between Te and non-bridging oxygen (NBO) atoms found on the [TeO<sub>3</sub>] and [TeO<sub>3+1</sub>] sites respectively. The ([TeO<sub>3</sub>]/[TeO<sub>3+1</sub>]) units can be thought of as distorted [TeO<sub>4</sub>] tbp units, with one oxygen further away from the central tellurium than the remaining three

oxygen.

The typical transmittance spectra of a silver-containing tellurite glass is displayed in Fig. 4a (glass TZ[Na<sub>8</sub>Ag<sub>2</sub>], thickness,  $t = 1.70$  mm). The glass samples were of yellow color and they turned dark red with increasing Ag<sub>2</sub>O content (inset). Tellurite-based glasses have a long optical window up to 6  $\mu\text{m}$ . Absorption bands around 3  $\mu\text{m}$  are clearly correlated with the presence of hydroxyl groups in the glass structure ( $-\text{OH}$ ,  $\text{H}_2\text{O}$ ,  $\text{TeOH}\dots$ ), hence limiting the transmission in the near-IR region. This is due to the fact that no specific purification protocol beside the use of high-purity precursors was introduced at this stage of the study.

The absorption spectra of the glasses TZ[Na<sub>10-x</sub>Ag<sub>x</sub>] are depicted in Fig. 4b. The cut-off wavelength of the glasses ( $\lambda_c$ ) have been extracted from the absorption coefficient plot for  $\alpha = 10$   $\text{cm}^{-1}$ . It shows a red-shifted absorption edge with gradual Ag<sub>2</sub>O insertion, from  $\lambda_c = 370$  nm for  $x = 0\%$  to  $\lambda_c = 505$  nm for  $x = 10\%$ .

The refractive index evolution with silver content are plotted for the 633, 1064 and 1550 nm wavelengths on Fig. 5a. The refractive index increases monotonously with increasing Ag<sub>2</sub>O content, from  $n = 2.05$  ( $x = 0\%$ ) to  $n = 2.16$  ( $x = 10\%$ ) at 633 nm. The materials dispersion on wavelength can be further analyzed through the Sellmeier equation (Fig. 5b). The wavelength-dependent refractive index curve for each glass was determined with the following one-pole Sellmeier equation (Eq. 1):

$$n^2 = A + \frac{B\lambda^2}{\lambda^2 - C^2} \quad (1)$$

where  $\lambda$  is the wavelength and  $A$ ,  $B$ , and  $C$  are the Sellmeier coefficients obtained by a least-square fitting procedure, applied to measured refractive indices  $n$ . No evolution with  $x$  of the dispersion can be observed, traducing the fact that the main resonance associated with the dispersion evolution in the UV range remains constant.

The contamination of the TZ[Na<sub>10-x</sub>Ag<sub>x</sub>] glasses with platinum has been evidenced by ICO-OES (Fig. 6). The silver-free TZN glass contains the lowest concentration in platinum (0.02% in weight). As silver oxide is introduced, the platinum content increases sharply, up to 0.79% for  $x = 10$ . At such a high concentration, platinum might be not be considered as a contaminant anymore but as a doping element of the glass. The metal penetrates the glass because of an erosive and corrosive action of the fluid glass mass on the crucible. The ICO-OES analysis highlights the fact in addition to this effect, the silver affects strongly the interaction between the melt and the platinum crucible.

Luminescence spectroscopy have been conducted on the different glasses. The Fig. 7 reports the emission and excitation spectra recorded respectively for excitation at 360 nm and emission at around 680 nm of the TZN glass without silver ions ( $x = 0$ ) fabricated in platinum crucible.

A weak red emission centered around 700 nm can be observed for all glass compositions prepared in platinum crucible (Fig. 7). One have to notice that such emission is not appearing in TZ[Na<sub>10-x</sub>Ag<sub>x</sub>] glasses prepared in gold crucible for comparison (not presented here). Corresponding to this emission band, a broad excitation spectrum for emission at around 680 nm is observed from 320 nm to 550 nm with two maxima at around 370 nm and 475 nm.

For all silver containing glasses fabricated in platinum crucible, a similar emission band peaking at around 700 nm can be observed for excitation between 350 nm up to 470 nm (Fig. 8a). The emission signal strongly decreases with the introduction of the silver oxide in the glass composition. Although special care has been taken to correct the spectra using a white calibrated lamp, one believe that the weak shift of the emission band occurring in a spectral region not optimal for the detection system (observed in particular for the sample  $x = 8$ ) is mainly related to the correction procedure. The Fig. 8b depicts the different excitation spectra collected for  $x = 2, 6$  and  $10$ . As compared to the excitation spectrum collected for  $x = 0$  (Fig. 7), the introduction of silver leads to a broadening of spectra with an excitation band between 450 nm and 550 nm with the presence of a new contribution at around 500 nm as the silver concentration increases. The relative intensity of this band increases with the increase of the silver content. Nevertheless, one have to notice that such new contribution leads to the same emission spectrum traducing that the center responsible for the emission remains the same.

## 4. Discussion

Here one investigated the influence of the substitution between the modifiers compounds  $\text{Na}_2\text{O}$  and  $\text{Ag}_2\text{O}$  on the properties of the tellurite glasses in the system  $\text{TeO}_2\text{-ZnO-Na}_2\text{O-Ag}_2\text{O}$ . Raman measurements (Fig. 3) suggests that the progressive substitution of sodium by silver do not lead to a drastic change in the basic structure of the  $\text{TZ}[\text{Na}_{10-x}\text{Ag}_x]$  glass network. The relative intensity of the bands at  $450\text{ cm}^{-1}$  and  $610\text{ cm}^{-1}$  remain nearly constant with the progressive substitution of  $\text{Na}_2\text{O}$  by  $\text{Ag}_2\text{O}$ , while the high-frequency shoulder (centered on the bands at  $715$  and  $775\text{ cm}^{-1}$ ) is slightly shifted toward the lower frequencies. The high-frequency broad shoulder contains two main contributions generally assigned to stretching modes of  $[\text{TeO}_{3+1}]$  and  $[\text{TeO}_3]$  units, which maximum position depends on the nature of counter cations. One expect that with sodium ions depletion the remaining NBO atoms would be compensated by silver ions. The large electro-negativity difference between sodium and silver ions ( $\chi_{\text{Na}} = 0.93$ ,  $\chi_{\text{Ag}} = 1.93$ ) implies that  $\text{Ag}^+$  ions have a larger tendency than  $\text{Na}^+$  ions to form covalent bonds with oxygen atoms ( $\chi_{\text{O}} = 3.44$ ). Under this assumption, the observed spectral shift could be associated with a decrease of the ionic character of the bonds between tellurite and NBO, in connection with the decrease of the net cation charge arising from the substitution of sodium by silver.

Although the equimolar substitution between  $\text{Na}_2\text{O}$  and  $\text{Ag}_2\text{O}$  oxide modifiers does not lead to a meaningful evolution in the structure of the  $\text{TZ}[\text{Na}_{10-x}\text{Ag}_x]$  glass network, it alters substantially their properties. The density of the glasses  $\text{TZ}[\text{Na}_{10-x}\text{Ag}_x]$  increases linearly with  $x$  (Fig. 2b). This evolution is attributed to the progressive substitution of sodium oxide by silver oxide with a significantly higher molar mass ( $M_{\text{Na}_2\text{O}} = 61.98\text{ g.mol}^{-1}$  and  $M_{\text{Ag}_2\text{O}} = 231.74\text{ g.mol}^{-1}$  respectively). The thermal analysis of the glasses  $\text{TZ}[\text{Na}_{10-x}\text{Ag}_x]$  shows that silver insertion causes a slight, monotonous decrease of the  $T_g$  as well as of the resistance to crystallization of the glass network (Fig. 2a). According to the large difference in electronegativity between  $\text{Na}^+$  ions by  $\text{Ag}^+$  ions, the covalence of the bonds between NBOs and monovalent cations is expected to increase. This process is expected to cause an increase in the glass transition temperature of the mixed modifier tellurite glasses with  $x$ . This assumption is reinforced by the increase of the overall glass network connectivity upon replacing  $\text{Na}_2\text{O}$  by  $\text{Ag}_2\text{O}$ . However, although such an increase of the  $T_g$  with alkali/silver substitution was partially observed by G. El-Damrawi [[34]] other works, similarly to our observation, mentioned a decrease of the  $T_g$  [[35],[36]]. The variation in the glass transition temperature in glasses can be ascribed to trade-off between multiple factors such as glass network structural changes, average cross-link density, bonds strength and concentration, average stretching force. For both bulk and powder samples, silver induces a decrease of the onset crystallization peaks, which emphasizes the role of  $\text{Ag}_2\text{O}$  as nucleating agent to facilitate the crystallization. This observation is in good agreement with previous observation made in niobium oxide glasses [[30]]. However, unlike previous observation made in germane-tellurite glasses [[20]], the effect of silver oxide as nucleating agent to promote bulk versus surface crystallization was not evidenced.

When comparing with the TZN glass, one observe (Fig. 5a) a steady increase of the refractive index with the progressive substitution of sodium by silver ions, this increase being as high as  $\Delta n \simeq +0.1$  for  $x = 10\%$ . Such variation of the refractive index with silver oxide content is consistent with previous observation made in other tellurite glass systems [[17],[19],[31]]. The increase of the refractive index results from an increase of the average electronic polarizability of the glass with the  $\text{Na}^+ \rightarrow \text{Ag}^+$  substitution, which global contribution results from the polarizabilities of the individual constituting ions of the glass ( $\alpha_{\text{Na}^+} = 0.18\text{ \AA}^3$  [[32]],  $\alpha_{\text{Ag}^+} = 1.7\text{-}2.2\text{ \AA}^3$  [[19],[33]]).

The cut-off wavelength of the glasses shows a red-shifted absorption edge with gradual  $\text{Ag}_2\text{O}$  insertion, from  $\lambda_c = 356\text{ nm}$  for  $x = 0\%$  to  $\lambda_c = 505\text{ nm}$  for  $x = 10\%$ . This is in good agreement with previous observation made in other systems such as in silver-containing  $\text{TeO}_2\text{-WO}_3\text{-La}_2\text{O}_3$  glasses [[21]]. One suggest that the absorption edge shifts to the longer wavelength is probably due to the broadening of the valence band as a result of the strong coupling of  $\text{Ag}^+d$ -electron orbitals with  $\text{O}^{2-}p$ -electron orbitals. It results in an extension of the localized states within the gap and a decrease in optical band-gap energy. Yet, regarding the evolution of the cut-off wavelength at the limit of the UV/visible range, precaution need to be taken. Glasses prepared in platinum crucible exhibit yellowish color as compared to glasses prepared in gold crucible. Platinum has certainly a strong effect on the absorption feature of the  $\text{TZ}[\text{Na}_{10-x}\text{Ag}_x]$  glasses in the visible range. Moreover, an emission band centered at  $700\text{ nm}$  for excitation between  $320\text{ nm}$  up to  $500\text{ nm}$  can be detected for all glasses made in platinum crucible (Fig. 7, Fig. 8). As revealed by ICP-OES analysis (Fig. 6), the platinum concentration is strongly affected by the content of silver oxide in the composition, silver ions favoring the introduction of the platinum in the composition to reach up to  $0.8\text{ wt}\%$  for  $x = 10$ . In the glass, platinum may be introduced as  $\text{Pt}^0$ ,  $\text{Pt}^{2+}$  and/or  $\text{Pt}^{4+}$ . The presence of

metallic particles was discarded as no plasmon resonance effect was detected in the glass.  $\text{Pt}^{2+}$  and  $\text{Pt}^{4+}$  cations possess a  $d^8$  and  $d^6$  electronic configuration respectively. Absorption of such cations are generally located in the visible [[37],[38]], which is in good agreement with the two absorption bands detected on the excitation spectra of silver doped glasses  $x = 2, 6$  and  $10$  on Fig. 8b. Here, due to the overlap between the absorption of the glass matrix and of the platinum cations, it will be difficult to conclude on the oxidation state of metallic species  $\text{Pt}^{2+}$  or  $\text{Pt}^{4+}$ . Yet, the assumption for the presence of the  $\text{Pt}^{4+}$  species is generally highly supported by experiments [[22],[37],[39]]. When the silver content increases, new contributions appear in the excitation spectra at around  $500\text{ nm}$ , while in the meantime the emission spectrum remains the same. We believe this evolution is mainly responsible for the red shift of the absorption edge of the tellurite glasses observed on Fig. 4b. One assume at this stage a strong interaction between the platinum crucible and the tellurite ions. It was already evidenced in the growth of  $\text{TeO}_2$  crystals melted in platinum container, leading to the occurrence of striations, black inclusions and gas bubbles [[40]]. J. Mangin et al. proposed that the mechanism of dissociation of  $\text{Te}-\text{O}$  bonds proceeds from the intermediate formation of platinum telluride compounds. In addition, one observed that the increase in silver induces a higher corrosion on the platinum crucible. At this stage, it is not straightforward to elucidate the origin of the catalytic effect of silver on the dissolution rate of metallic platinum. The direct reaction between metallic Pt and  $\text{Ag}^+$  silver ions is not supported by electrochemical potentials. Hence one assume that silver affects the glass melt (i.e. acido-basicity of the melt, mass transport diffusion due to the wettability of the glass...), which in turn led to a higher reactivity with platinum. The progressive oxidation of platinum by the melt could induce the reduction of silver or tellurium ions and formation of compounds in the  $\text{Te}-\text{Ag}$  system, which could lead to the optical absorption observed at  $\sim 500\text{ nm}$ . One can suspect that such compound in the  $\text{Ag}-\text{Te}$  system could be highly sensitive to oxidation when the melting temperature is increased. The luminescence of platinum cations drops drastically with the increase of silver in the glass. This could be due either to a competitive absorption of the compounds absorbing near  $500\text{ nm}$  or a possible concentration quenching effect. Further analysis are necessary to elucidate the increase of solubility of Pt in silver containing tellurite glass, and to identify the absorbing species existing into the melt.

Although the progressive equimolar substitution between  $\text{Na}_2\text{O}$  and  $\text{Ag}_2\text{O}$  oxides does not lead to a meaningful evolution in the structure of the  $\text{TZ}[\text{Na}_{10-x}\text{Ag}_x]$  glass network, it enables fine-tuning the glass transition temperature, density, refractive index and cut-off wavelength of the investigated glasses over a broad range of composition, such properties being desired for the design of specific waveguides components. The silver atom size, charge and polarizability contribute strongly into the observed modifications. Structural investigations will be required to probe the exact electrostatic influence of silver ions on the glass structures and properties and discriminate potential mixing effects between cation ions.

## 5. Conclusion

Here one examined the influence of the substitution of modifier oxides  $\text{Na}_2\text{O}$  by  $\text{Ag}_2\text{O}$  on the platinum contamination and properties of glasses in the system  $\text{TeO}_2-\text{ZnO}-\text{Na}_2\text{O}-\text{Ag}_2\text{O}$ . Results highlight a clear correlation between the silver content, the glass network structure and the corresponding properties of the material. The variation of glass transition temperature decreases linearly with silver content whereas the surface crystallization mechanism is favored. Furthermore one observe a large increase in the linear refractive index and a red-shift in the optical band gap with  $\text{Ag}_2\text{O}$  content. Raman spectroscopy do not suggest a strong evolution in the tellurite network connectivity with  $\text{Ag}_2\text{O}$  insertion but instead a modification in the iono-covalency of the bonds. Factors such as the silver atoms size, charge and polarizability appear to contribute mainly into the observed modification of the properties of the glasses. Finally, we demonstrate that silver ions strongly exacerbate the interaction between the platinum from the crucible and the glass melt during synthesis, leading to glasses containing up to  $0.8\%$  in weight of Pt. Silver-containing tellurite glass materials could be very attractive candidates in bulk or fiber forms for photonic or in nonlinear optics where strong confinement of light and promoted effective nonlinear effects are needed.

## Acknowledgements

This project has received funding from the European Union's Horizon 2020 research and innovation programme under the Marie Skłodowska-Curie grant agreement No 823941 (FUNGLASS). Funding for this work has been provided from the French Government, managed by the French National Research Agency (ANR Grant #58533), by the Programme IdEx at the University of Bordeaux, the Cluster of excellence LAPHIA and by the Aquitaine Region.

## References

- [1] J.S. WANG, E.M. VOGEL, E. SNITZER. TELLURITE GLASS: A NEW CANDIDATE FOR FIBER DEVICES. *OPT. MATER.*, 3 (1994), p. 187.
- [2] R.H. EL-MALLAWANY. TELLURITE GLASSES HAND BOOK – PHYSICAL PROPERTIES AND DATA, CRC PRESS LLC (2002).
- [3] W.C. WANG, W.J. ZHANG, L.X. LI, Y. LIU, D.D. CHEN, Q. QIAN, Q.Y. ZHANG. SPECTROSCOPIC AND STRUCTURAL CHARACTERIZATION OF BARIUM TELLURITE GLASS FIBERS FOR MID-INFRARED ULTRA-BROAD TUNABLE FIBER LASERS. *OPT. MATER. EXPRESS*, 6 (2016), p. 2095.
- [4] R. STEGEMAN, C. RIVERO, K. RICHARDSON, G. STEGEMAN, P. DELFYETT, Y. GUO, A. POPE, A. SCHULTE, T. CARDINAL, P. THOMAS, J.-C. CHAMPARNAUD-MESJARD. RAMAN GAIN MEASUREMENTS OF THALLIUM-TELLURIUM OXIDE GLASSES. *OPT. EXPRESS*, 13 (2005), p. 1144.
- [5] A. LIN, A. ZHANG, E.J. BUSHONG, J. TOULOUSE. SOLID-CORE TELLURITE GLASS FIBER FOR INFRARED AND NONLINEAR APPLICATIONS. *OPT. EXPRESS*, 17 (2009), ARTICLE 16716.
- [6] S. MANNING, H. EBENDORFF-HEIDEPRIEM, T.M. MONRO. TERNARY TELLURITE GLASSES FOR THE FABRICATION OF NONLINEAR OPTICAL FIBRES. *OPT. MATER. EXPRESS*, 2 (2012), p. 140.
- [7] C. STRUTYNSKI, F. DESEVEDAVY, A. LEMIÈRE, J.-C. JULES, G. GADRET, T. CARDINAL, F. SMEKTALA, S. DANTO. TELLURITE-BASED CORE-CLAD DUAL-ELECTRODES COMPOSITE FIBERS. *OPT. MATER. EXPRESS*, 7 (2017), p. 1503.
- [8] I. SAVELII, J.C. JULES, G. GADRET, B. KIBLER, J. FATOME, M. EL-AMRAOUI, N. MANIKANDAN, X. ZHENG, F. DÉSÉVEDAVY, J.M. DUDLEY, J. TROLES, L. BRILLAND, G. RENVERSEZ, F. SMEKTALA. SUSPENDED CORE TELLURITE GLASS OPTICAL FIBERS FOR INFRARED SUPERCONTINUUM GENERATION. *OPT. MATER.*, 33 (2011), p. 1661.
- [9] C. STRUTYNSKI, J. PICOT-CLÉMENTE, A. LEMIÈRE, P. FROIDEVAUX, F. DÉSÉVEDAVY, G. GADRET, J.-C. JULES, B. KIBLER, F. SMEKTALA. FABRICATION AND CHARACTERIZATION OF STEP-INDEX TELLURITE FIBERS WITH VARYING NUMERICAL APERTURE FOR NEAR- AND MID-INFRARED NONLINEAR OPTICS. *J. OPT. SOC. AM. B*, 31 (2016), p. 0740.
- [10] M. FRUMAR, T. WAGNER. DOPED CHALCOGENIDE GLASSES AND THEIR APPLICATIONS. *CURR. OPINION SOLID STATE MATER. SCI.*, 7 (2003), p. 117.
- [11] S. DANTO, F. DÉSÉVEDAVY, Y. PETIT, J.-C. DESMOULIN, A. ABOU KHALIL, C. STRUTYNSKI, M. DUSSAUZE, F. SMEKTALA, T. CARDINAL, L. CANIONI. PHOTO-WRITABLE SILVER-CONTAINING PHOSPHATE GLASS RIBBON FIBERS. *ADV. OPT. MATER.*, 4 (2016), p. 162.
- [12] A. ROYON, K. BOURHIS, M. BELLEC, G. PAPON, B. BOUSQUET, Y. DESHAYES, T. CARDINAL, L. CANIONI. SILVER CLUSTERS EMBEDDED IN GLASS AS A PERENNIAL HIGH CAPACITY OPTICAL RECORDING MEDIUM. *ADV. MATER.*, 22 (2010), p. 5282.
- [13] Y. MIYAMOTO, Y. TAKEI, H. NANTO, T. KUROBORI, A. KONNAI, T. YANAGIDA, A. YOSHIKAWA, Y. SHIMOTSUMA, M. SAKAKURA, K. MIURA, K. HIRAO, Y. NAGASHIMA, T. YAMAMOTO. RADIOPHOTOLUMINESCENCE FROM SILVER-DOPED PHOSPHATE GLASS. *RADIAT. MEAS.*, 46 (2011), p. 1480.
- [14] L.R.P. KASSAB, C.B. DE ARAÚJO, R.A. KOBAYASHI, R.A. PINTO, D.M. DA SILVA. INFLUENCE OF SILVER NANOPARTICLES IN THE LUMINESCENCE EFFICIENCY OF Pr<sup>3+</sup>-DOPED TELLURITE GLASSES. *J. APPL. PHYS.*, 102 (2007), ARTICLE 103515.
- [15] L.P.R. KASSAB, L.F. FREITAS, K. OZGA, M.G. BRIK, A. WOJCIECHOWSKI. ZNO-TEO<sub>2</sub>-Yb/TM GLASSES WITH SILVER NANOPARTICLES AS LASER OPERATED QUANTUM ELECTRONIC DEVICES. *OPT. LASER TECHNOL.*, 42 (2010), p. 1340.
- [16] L.R.P. KASSAB, R. DE ALMEIDA, D.M. DA SILVA, C.B. DE ARAÚJO. LUMINESCENCE OF Tb<sup>3+</sup> DOPED TeO<sub>2</sub>-ZnO- Na<sub>2</sub>O-PbO GLASSES CONTAINING SILVER NANOPARTICLES. *J. APPL. PHYS.*, 104 (2008), ARTICLE 093531.
- [17] J.M. GIEHL, W.M. PONTUSCHKA, L.C. BARBOSA, E.F. CHILLCCE, Z.M. DA COSTA, S. ALVES. THERMAL PRECIPITATION OF SILVER NANOPARTICLES AND THERMOLUMINESCENCE IN TELLURITE GLASSES. *OPT. MATER.*, 33 (2011), p. 1884.
- [18] S. UKON, S. KAWASE, S. MURAI, K. FUJITA, K. TANAKA. SURFACE MODIFICATION OF TELLURITE GLASS BY THERMAL POLING ACCOMPANIED WITH ION IMPLANTATION IN A SOLID-STATE PHASE. *PHYS. CHEM. GLASSES EUR. J. GLASS SCI. TECHNOL. B*, 49 (2008), p. 285.
- [19] D. LINDA, J.-R. DUCLÈRE, T. HAYAKAWA, M. DUTREILH-COLAS, T. CARDINAL, A. MIRGORODSKY, A. KABADOU, P. THOMAS. OPTICAL PROPERTIES OF TELLURITE GLASSES ELABORATED WITHIN THE TeO<sub>2</sub>-Tl<sub>2</sub>O-Ag<sub>2</sub>O AND TeO<sub>2</sub>-ZnO-Ag<sub>2</sub>O TERNARY SYSTEMS. *J. ALLOYS AND COMPOUNDS*, 561 (2013), p. 151.
- [20] L.N. TRUONG, M. DUSSAUZE, M. ALLIX, S. CHENU, T. CARDINAL, E. FARGIN, L.F. SANTOS. SECOND HARMONIC GENERATION IN GERMANOTELLURITE BULK GLASS-CERAMICS. *J. AM. CERAM. SOC.*, 100 (2017), p. 1412.
- [21] B.S. STEPANOV, M.E. SHENINA, I.V. ANTONOV, M.F. CHURBANOV. EFFECT OF SILVER AND SODIUM IONS ON THE REFRACTIVE INDEX AND STRUCTURE OF TeO<sub>2</sub>-WO<sub>3</sub>-La<sub>2</sub>O<sub>3</sub> GLASSES. *INORG. MATER.*, 51 (2015), p. 811.
- [22] R.J. GINTHER. THE CONTAMINATION OF GLASS BY PLATINUM. *J. NON-CRYSTAL. SOLIDS*, 6 (1971), p. 294.
- [23] S. JIANG, Y. JIANG, D. ZHUO. PLATINUM POLLUTION IN PHOSPHATE LASER GLASSES. *CHINESE JR. LASERS*, 18 (1991), p. 913.
- [24] J. CAMPBELL, E.P. WALLERSTEIN, H. TORATANI, H. MEISSHER, S. NAKAJIMA, T.S. IZUMITANI. EFFECTS OF PROCESS GAS ENVIRONMENT ON PLATINUM-INCLUSION DENSITY AND DISSOLUTION RATE IN PHOSPHATE LASER GLASSES. *GLASS SCI. TECHNOL. FRANKFURT*, 68 (1995), p. 59.
- [25] D. PALLES, I. KONIDAKIS, C.P.E. VARSAMIS, E.I. KAMITSOS. VIBRATIONAL SPECTROSCOPIC AND BOND VALENCE STUDY OF STRUCTURE AND BONDING IN Al<sub>2</sub>O<sub>3</sub>-CONTAINING AgI-AgPO<sub>3</sub> GLASSES. *RSC ADV.*, 6 (2016), ARTICLE 16697.
- [26] F. FARGES, D.R. NEUVILLE, G.E. BROWN JR. STRUCTURAL INVESTIGATION OF PLATINUM SOLUBILITY IN SILICATE GLASSES. *AM. MINERAL.*, 84 (1999), p. 1562.
- [27] V.V. DOROFEEV, A.N. MOISEEV, M.F. CHURBANOV, T.V. KOTEREVA, A.V. CHILYASOV, I.A. KRAEV, V.G. PIMENOV, L.A. KETKOVA, E.M. DIANOV, V.G. PLOTNICHENKO, A.F. KOSOLAPOV, V.V. KOLTASHEV. PRODUCTION AND PROPERTIES OF HIGH PURITY TeO<sub>2</sub>-WO<sub>3</sub>-(La<sub>2</sub>O<sub>3</sub>, Bi<sub>2</sub>O<sub>3</sub>) AND TeO<sub>2</sub>-ZnO-Na<sub>2</sub>O-Bi<sub>2</sub>O<sub>3</sub> GLASSES. *J. NON-CRYSTAL. SOLIDS*, 357 (2011), p. 2366.
- [28] K. KATO, T. HAYAKAWA, Y. KASUYA, P. THOMAS. INFLUENCE OF Al<sub>2</sub>O<sub>3</sub> INCORPORATION ON THE THIRD-ORDER NONLINEAR OPTICAL PROPERTIES OF Ag<sub>2</sub>O-TeO<sub>2</sub> GLASSES. *J. NON-CRYSTAL. SOLIDS*, 431 (2016), p. 97.
- [29] M.F. CHURBANOV, G.E. SNOPATIN, E.V. ZORIN, S.V. SMETANIN, E.M. DIANOV, V.G. PLOTNICHENKO, V.V. KOLTASHEV, E.B. KRYUKOVA, I.A. GRISHIN, G.G. BUTSIN. GLASSES OF TeO<sub>2</sub>-WO<sub>3</sub> AND TeO<sub>2</sub>-WO<sub>3</sub>-La<sub>2</sub>O<sub>3</sub> SYSTEMS FOR FIBER OPTICS. *J. OPTOELECTRON. ADV. MATER.*, 7 (2005), p. 1765.
- [30] H. SMOGOR, T. CARDINAL, V. JUBERA, E. FARGIN, J.J. VIDEAU, S. GOMEZ, R. GRODSKY, T. DENTON, M. COUZI, M. DUSSAUZE. EFFECT OF SILVER ON PHASE SEPARATION AND CRYSTALLIZATION OF NIOBIUM OXIDE CONTAINING GLASSES. *J. SOLID STATE CHEM.*, 182 (2009), p. 1351.
- [31] G. UPENDER, S. RAMESH, M. PRASAD, V.G. SATHE, V.C. MOULI. OPTICAL BAND GAP, GLASS TRANSITION TEMPERATURE AND STRUCTURAL STUDIES OF (100-2x)TeO<sub>2</sub>-xAg<sub>2</sub>O-xWO<sub>3</sub> GLASS SYSTEM. *J. ALLOYS COMPD.*, 504 (2010), p. 468.
- [32] R. EL-MALLAWANY. THE OPTICAL PROPERTIES OF TELLURITE GLASSES. *J. APPL. PHYS.*, 72 (1992), p. 1774.
- [33] J.A. DUFFY, B. HARRIS, E.I. KAMITSOS, G.D. CHRISIKOS, J.A. KAPOUTSIS. POLARISING POWER AND POLARISABILITY OF THE Ag<sup>+</sup> ION IN GLASS: THE BASICITY OF SILVER(I) OXIDE. *PHYS. CHEM. GLASSES*, 39 (1998), p. 275.
- [34] G. EL-DAMRAWI. MIXED MOBILE ION EFFECTS IN SOME TELLURITE AND PHOSPHOTELLURITE GLASS. *PHYS. CHEM. GLASSES*, 42 (2001), p. 56.
- [35] T. YANO, K. AZEGAMI, S. SHIBATA, M. YAMANE. CHEMICAL STATE OF OXYGEN IN Ag<sup>+</sup>/Na<sup>+</sup> ION-EXCHANGED SODIUM SILICATE GLASS. *J. NON-CRYST. SOLIDS*, 222

(1997), p. 94.

[36] M. YAMANE, S. SHIBATA, A. YASUMORI, T. YANO, H. TAKADA. STRUCTURAL EVOLUTION DURING  $Ag^+/Na^+$  ION EXCHANGE IN A SODIUM SILICATE GLASS. *J. NON-CRYST. SOLIDS*, 203 (1996), p. 268.

[37] C.A. CLICK, R.K. BROW, P.R. EHRMANN, J.H. CAMPBELL. CHARACTERIZATION OF  $Pt^{4+}$  IN ALUMINO-METAPHOSPHATE LASER GLASSES. *J. NON-CRYSTAL. SOLIDS*, 319 (2003), p. 95.

[38] J.M. BEVILACQUA, R. EISENBERG. SYNTHESIS AND CHARACTERIZATION OF LUMINESCENT SQUARE-PLANAR PLATINUM (II) COMPLEXES CONTAINING DITHIOLATE OR DITHIOCARBAMATE LIGANDS. *INORG. CHEM.*, 33 (1994), p. 2913.

[39] M. KARABULUT, G. KANISHKA MARASINGHE, C.A. CLICK, E. METWALLI, R.K. BROW, C.H. BOOTH, J.J. BUCHER, D.K. SHUH, T.I. SURATWALA, J.H. CAMPBELL. XAFS INVESTIGATION OF PLATINUM IMPURITIES IN PHOSPHATE GLASSES. *J. AM. CERAM. SOC.*, 85 (2002), ARTICLE 1093.

[40] J. MANGIN, P. VEBER.  $PtTe_2$ : POTENTIAL NEW MATERIAL FOR THE GROWTH OF DEFECT-FREE  $TeO_2$  SINGLE CRYSTALS. *J. CRYST. GROWTH*, 310 (2008), p. 3077.

**Table 1**  
Characteristic temperatures and density of the investigated glasses.

Sample	x (mol %)	Bulk		Powder			$\rho$ ( $\pm 0.02 \text{ g.cm}^{-3}$ )
		$T_g$ ( $\pm 3^\circ\text{C}$ )	$T_{x1\text{-Bulk}}$ ( $\pm 3^\circ\text{C}$ )	$T_g$ ( $\pm 3^\circ\text{C}$ )	$T_{x1\text{-Powder}}$ ( $\pm 3^\circ\text{C}$ )	$T_{x2\text{-Powder}}$ ( $\pm 3^\circ\text{C}$ )	
TZN	0	286	405	285	352	428	5.21
TZ[Na <sub>8</sub> Ag <sub>2</sub> ]	2	284	402	283	348	417	5.35
TZ[Na <sub>6</sub> Ag <sub>4</sub> ]	4	278	395	281	349	399	5.51
TZ[Na <sub>4</sub> Ag <sub>6</sub> ]	6	276	397	280	350	395	5.65
TZ[Na <sub>2</sub> Ag <sub>8</sub> ]	8	270	380	273	346	379	5.78
TZ[Na <sub>0</sub> Ag <sub>10</sub> ]	10	267	365	269	337	361	5.92

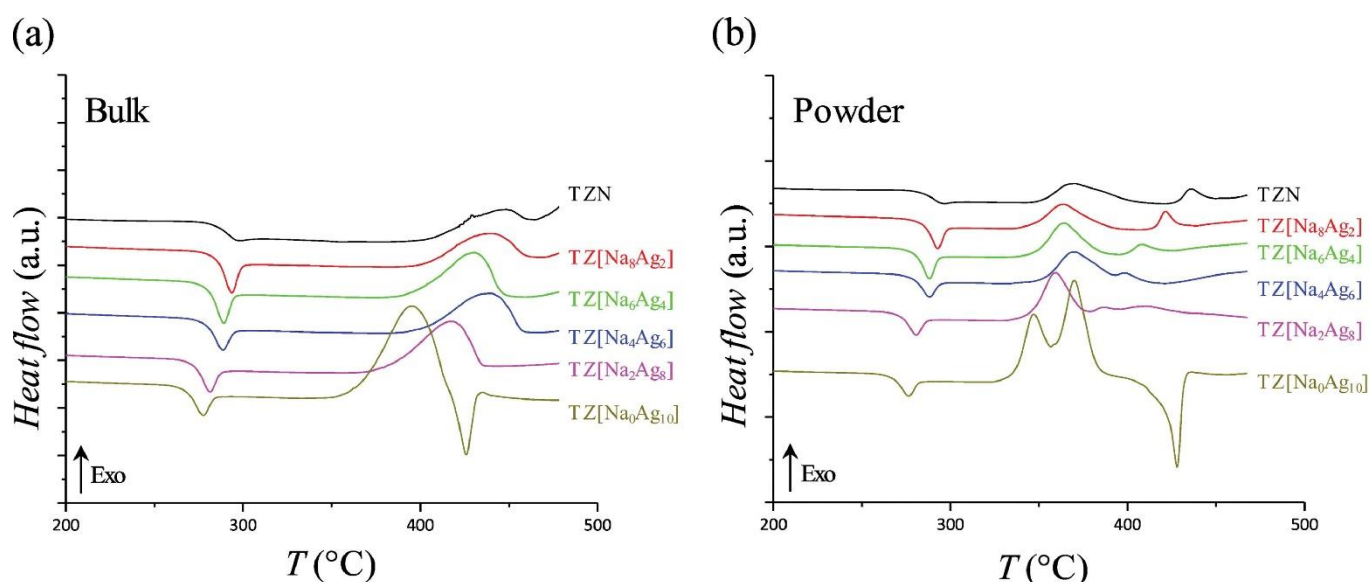


Fig. 1. DSC measurements of the glasses TZ[Na<sub>10-x</sub>Ag<sub>x</sub>] (a) Bulk (b) Powder.

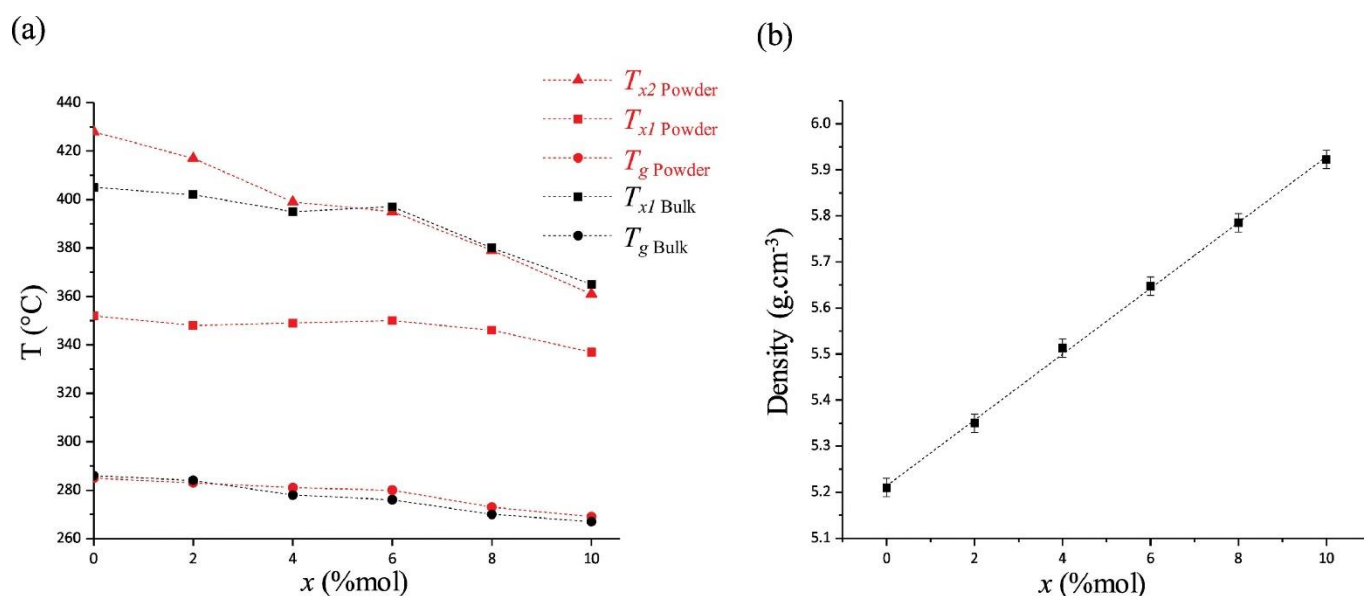


Fig. 2. (a) Evolution of the  $T_g$  and  $T_x$  and (b) of the density  $\rho$  of the glasses TZ[Na<sub>10-x</sub>Ag<sub>x</sub>] with silver content.

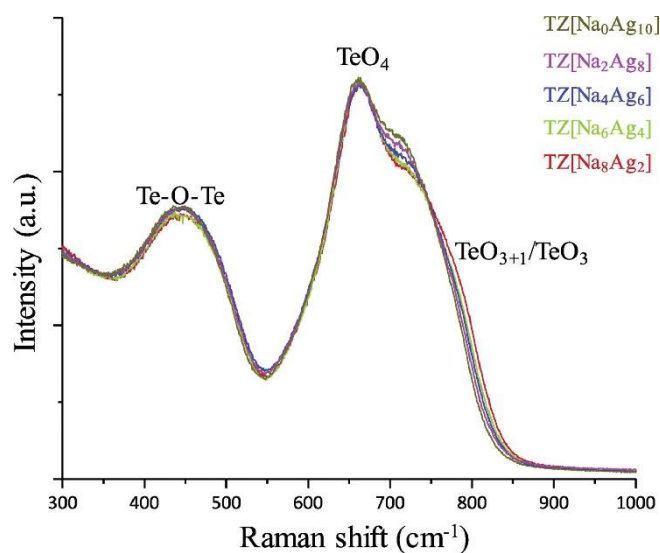


Fig. 3. Raman spectrum of the glasses TZ[Na<sub>10-x</sub>Ag<sub>x</sub>] ( $\lambda_{\text{Exc.}} = 785 \text{ nm}$ ).

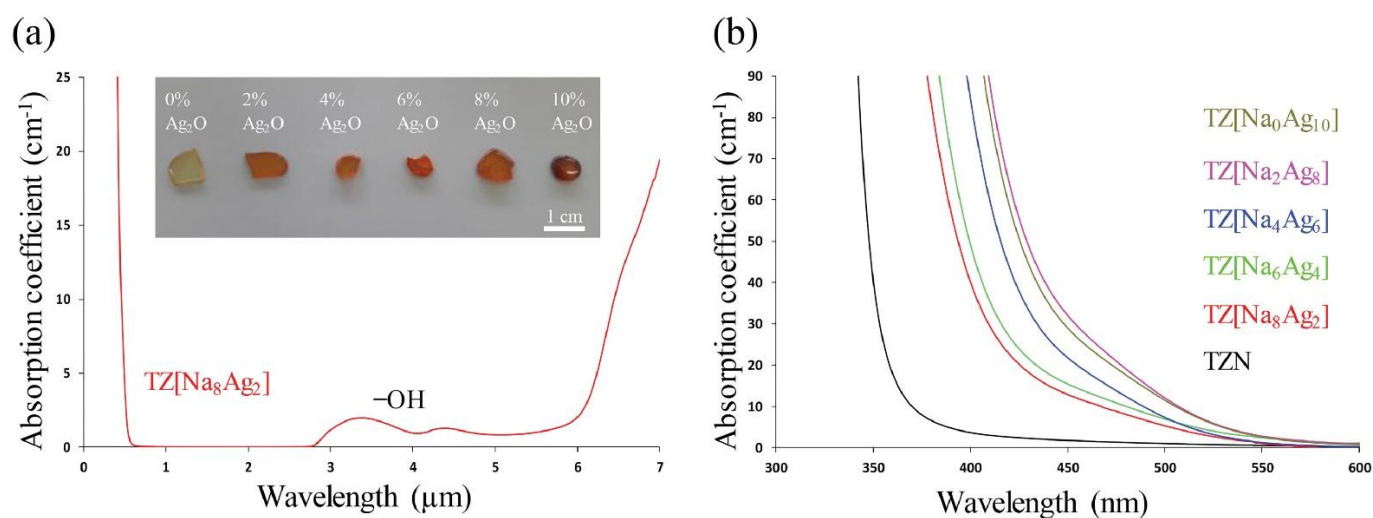


Fig. 4. (a) Absorption the glass TZ[Na<sub>8</sub>Ag<sub>2</sub>] ( $t = 1.70 \text{ mm}$ ) and (b) Absorption coefficient of the glasses TZ[Na<sub>10-x</sub>Ag<sub>x</sub>] with wavelength.

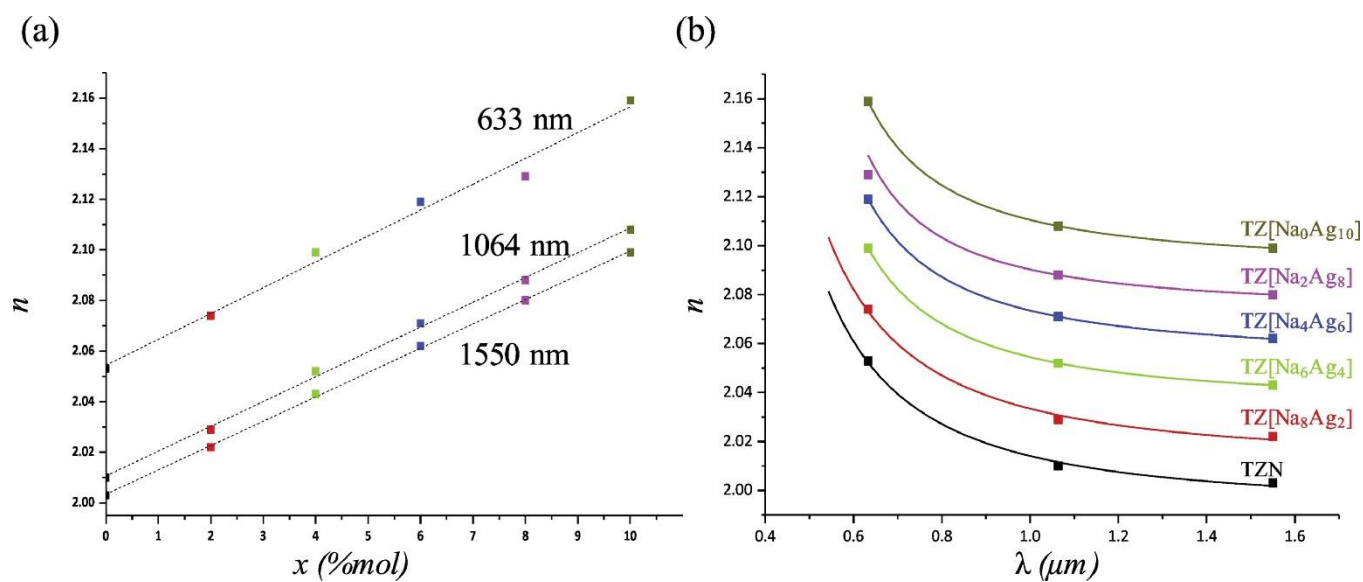


Fig. 5. (a) Refractive index of the glasses TZ[Na<sub>10-x</sub>Ag<sub>x</sub>] with  $x$  ( $\lambda = 633, 1064$  and  $1550$  nm) (b) Refractive index dispersion as a function of wavelength.

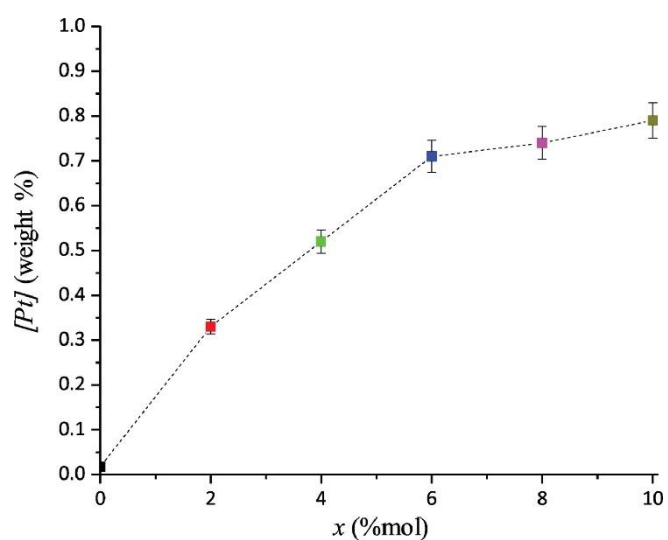


Fig. 6. Evolution of the platinum concentration with  $x$  (Ag content) measured by ICP-OES.

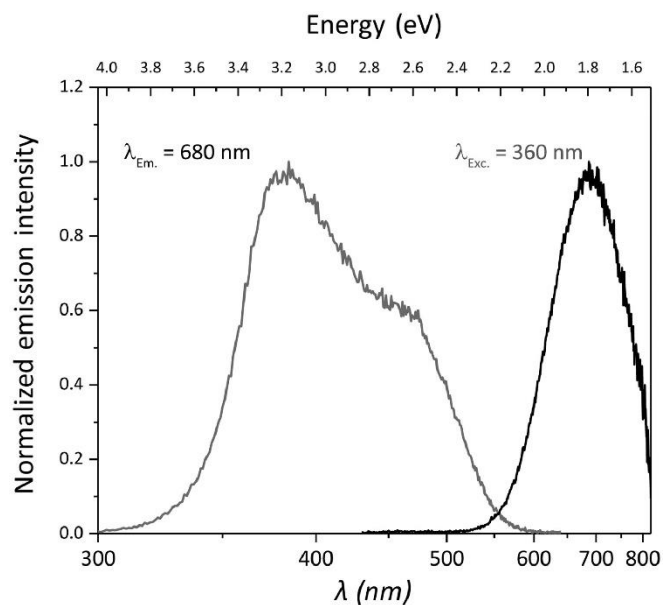


Fig. 7. Emission and excitation spectra of the TZN glass ( $x = 0$ ) fabricated in a platinum crucible collected respectively for excitation at 360 nm and emission at 680 nm.

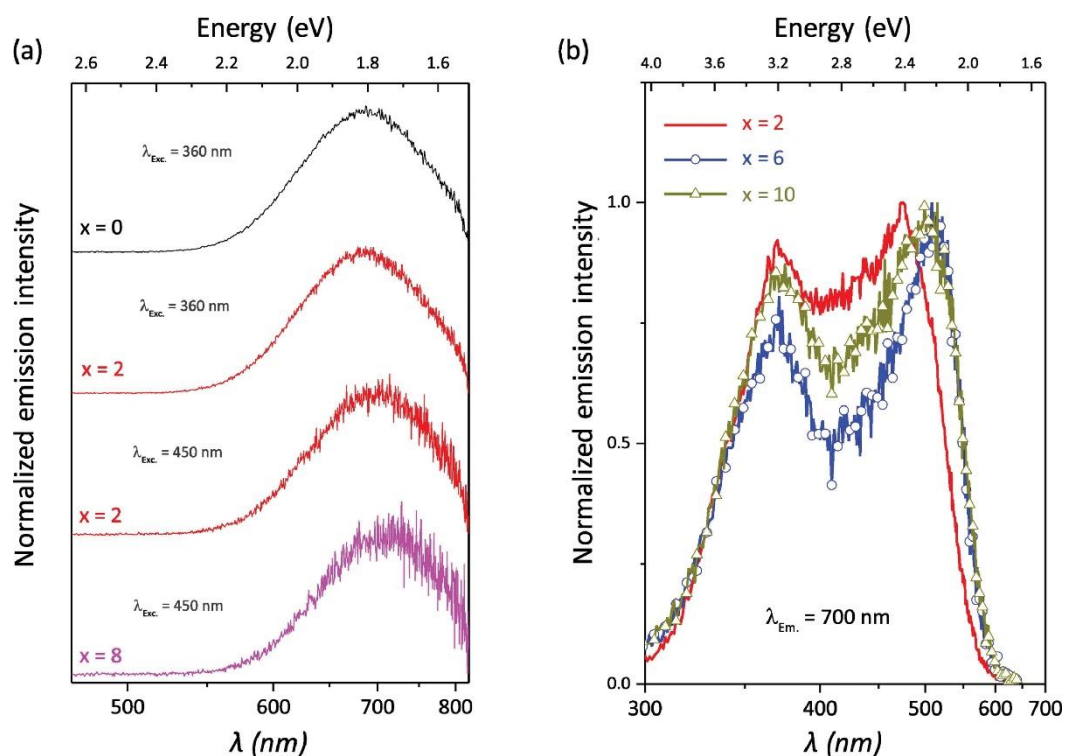


Fig. 8. (a) Emission spectra of the glasses  $x = 0, 2, 8$  for excitation at 360 nm or 450 nm (b) Normalized excitation spectra of the glasses  $x = 2, 6, 10$  for emission at 700 nm.